ARMA 18–202

Effects of Microfractures Properties on Stress-dependent Permeability in Tight Oil Reservoirs

Liu YANG*, Xiaobing LU

Key Laboratory for Mechanics in Fluid Solid Coupling Systems, Institute of Mechanics, Chinese Academy of Sciences, Beijing, China

Xian SHI, Kunheng ZHANG

China University of Petroleum (East China), Qingdao, China

Jian GAO, Xu CHEN, Zubo ZHANG

Research Institute of Petroleum Exploration and Development, Beijing, China

ABSTRACT: Several laboratory experiments are carried out to investigate the effects of microfractures on stress-dependent permeability. An analytical model depending on pore elasticity theory is proposed to study the related influencing factors. The results show that each curve of stress-dependent permeability is divided into two regions: microfractures closure region and pore compress region. The permeability decreases significantly in microfractures closure region, but it does not change too much in pore compress region. The permeability decreases by about 85~90% in total. It suggests that microfractures deformation cannot recover easily. The analytical solution results present that the volume fraction of microfractures has an important effect on stress-dependent permeability. The stress sensitive coefficient significantly decreases with the ratio of pores volume to microfractures volume (PV/FV). When the value of PV/FV is larger than 2, the stress sensitive coefficient does not change obviously with PV/FV. The high microfractures compressibility is the primary reason why the permeability in tight sandstone presents more sensitivity to effective stress.

1. INTRODUCTION

The exploration and development of tight oil is a hot topic following shale gas. The fast decline of production is observed during depletion development. It is essential to studying stress-dependent permeability for enhancing oil recovery. However, predicting the stress-dependent permeability is challenging due to the lack of pore change information at microscale. In addition, the tight sandstone is embedded by many microfractures that are easily compressed by effective stress (Chalmers et al., 2012). The changes of matrix pores and microfractures are synchronous under the effective stress, which compounds the difficulties in studying or predicting stress-dependent permeability.

The logarithmic empirical relationship is proposed to describe the relationship between fractured carbonates permeability and effective stress (Jones, 1975). Depending on Poiseuille’s equation, Walsh (1981) also represents the logarithmic relationship based on theoretical derivation procedure. As for fractured porous rocks, a polynomial relationship is derived to express the permeability with effective stress (Gangi, 1978). Dong et al. (2010) proposes that the power law relationship should be used to describe the stress-dependent permeability instead of the exponential relationship. The microfractures that are characterized by high pore compressibility cause strong stress sensitivity in tight oil reservoirs (Cho et al., 2013). In this study, several laboratory experiments are carried out to investigate the effects of microfractures on stress-dependent permeability. In addition, an analytical model is proposed to study the impacts of elastic modulus, Poisson’s ratio and microfractures volume fraction on stress sensitive coefficient.

2. EXPERIMENTS

2.1. Materials

The tight sandstone samples are collected from tight oil formation of Songliao Basin and Erdos Basin that are the greatest potential area for tight oil production. Considering the complex characteristics in tight oil reservoirs, the exploration and development of tight oil is still on the initial stage. The basic information is listed in table 1. The porosity of Fuyu and Chang-7 formation is 9.8% and 11.2%, respectively. The permeability of Fuyu and Chang-7 formation is 0.011mD and 0.003mD respectively. The permeability of Chang-7 formation is much smaller than Fuyu formation. The minerlogical compositions of two formations are listed in table 2.

They are characterized by low clay content and high quartz content.

In Fig. 1, the pictures of tight sandstone samples are listed. Fuyu formation sample does not contain microfractures. Two obvious microfractures are observed on the Chang-7 formation sample. The Scanning Electron Microscope (SEM) can help understand the pore structure of tight sandstone, as shown in Fig. 2. In Fuyu formation, the pore diameter is about 62~149 nm and no obvious fractures are found. In Chang-7 formation, the width of microfractures is about 124~253 nm. It is worth noting that the development of microfractures does not result in much larger permeability in Chang-7 formation.

The nuclear magnetic resonance equipment (MiniMR-VTP) can help analyze the pore size distribution, which is from Suzhou Niumag Analytical instrument Corporation. Two peaks of Chang-7 are presented in Fig. 3, which is consistent with the SEM observations. It can be explained by the microfractures in Chang-7 formation.

Table 1 Tight reservoir characteristics

Label	Formation	Source	Porosity (%)	Permeability (mD)
FY	Fuyu	Songliao Basin	9.8	0.011
C7	Chang-7	Erdos Basin	11.2	0.003

Table 2 The Minerlogical composition results

Label	Quartz	Calcite	Feldspar	Dolomite	Clay
FY	34.2	21.5	21.7	18.4	9.2
C7	32.0	15.1	18.7	20.5	13.7

(a)

(b)

Fig. 1 The pictures of tight sandstone samples: (a) Fuyu formation, (b) Chang-7 formation.

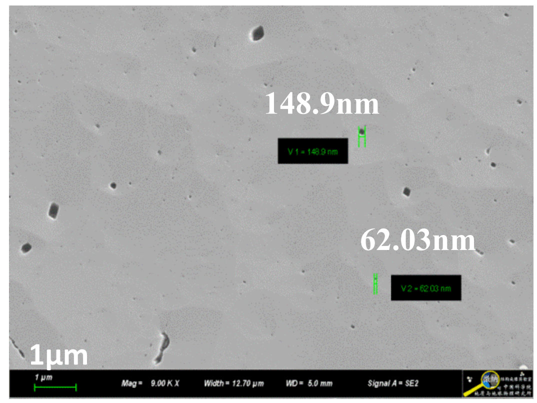

(a)

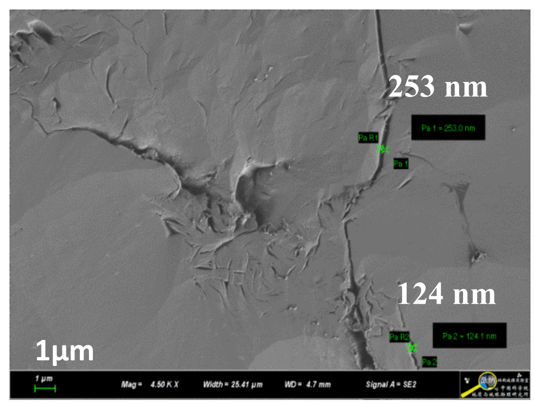

(b)

Fig. 2 The SEM pictures of tight sandstone samples: (a) Fuyu formation, (b) Chang-7 formation.

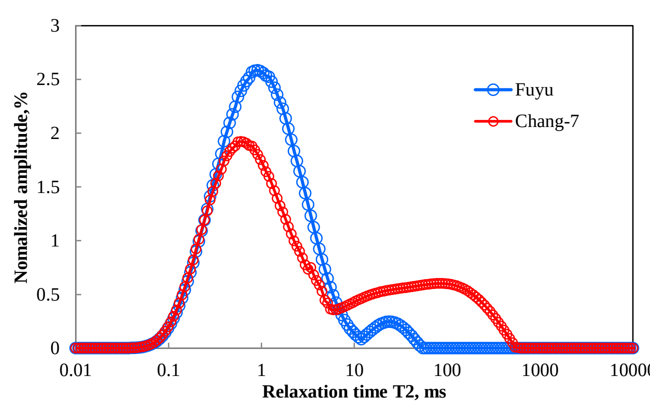

Fig. 3 The pore size distribution characteristics

2.2. Experimental procedure

In Fig. 4 and 5, the pictures of apparatus are listed. The setup composes of gas cylinder, core holder, pressure pump and gas-flow rate tester. The test temperature is about 25 ℃. The experimental procedure is as follows:

(1) Wash the samples using cleaning fluids and dry them for 48 hrs at the temperature of 105 ℃.

(2) Place the sample in the core holder. The confining pressure is 4 MPa, and the gas injection pressure is 0.25 MPa. The gas flow rate is recorded.

(3) Measure the gas flow rate at the confining pressure of 8, 12, 20, 30 and 40 MPa.

(4) Decrease the confining pressure to 30, 20, 12, 8 and 4 MPa successively, and record the gas flow rate.

(5) Calculate the permeability based on different gas flow rate and plot the curves of permeability vs. effective confining pressure.

Fig. 4 The set-up diagram for stress-dependent permeability.

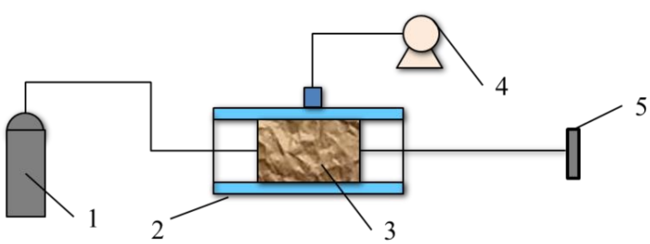

Fig. 5 Schematic illustration of apparatus. 1: gas cylinder; 2: core holder; 3: sample; 4: pressure pump; 5: gas-flow rate tester.

2.3. Experimental results

2.3.1 Fuyu formation samples

In Fig. 6, the relationship between permeability and effective confining pressure is presented in Fuyu formation. The permeability decreases gradually from ~0.016 mD to ~0.008 mD during the loading process, which results from pore compressibility. The confining pressure can compress the pore diameter to decrease the gas flow rate. The permeability increases gradually from ~0.008 mD to 0.011 mD during unloading process. It suggests that the compressed pores can recover due to pore elasticity (Reyes et al., 2002). However, they cannot recover completely, resulting from pore plasticity. So the final permeability is much lower than the initial permeability. The permeability damage degree of FY-1 and FY-2 sample is about 21% and 30% respectively.

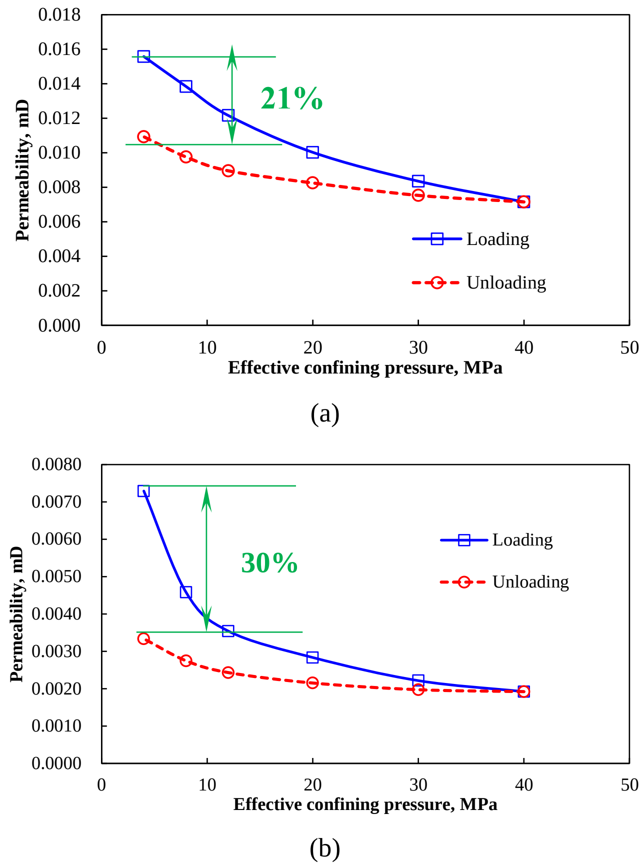

Fig. 6 The curves of permeability vs. confining pressure: (a) FY-1 sample, (b) FY-2 sample.

2.3.2 Chang-7 formation samples

In Fig. 7, the relationship between permeability and effective confining pressure is presented in Chang-7 formation. The permeability decreases gradually from ~0.0033 mD to ~0.0004 mD during the loading process. Two regions exist in the curves of Chang-7 formation, which is different from Fuyu formation. In the left region, a much sharper decline is observed in Chang-7 formation. It can be explained by the microfractures closure. In the right region, the permeability does not change too much, which is related to pores compression.

In addition, the permeability increases gradually from ~0.0004 mD to ~0.0006 mD during unloading process. The permeability damage degree of C7-1 and C7-2 sample is about 90% and 85% respectively. It suggests that microfractures deformation cannot recover easily. Therefore, the high microfractures compressibility is the primary reason why the permeability in tight sandstone presents more sensitivity to effective stress.

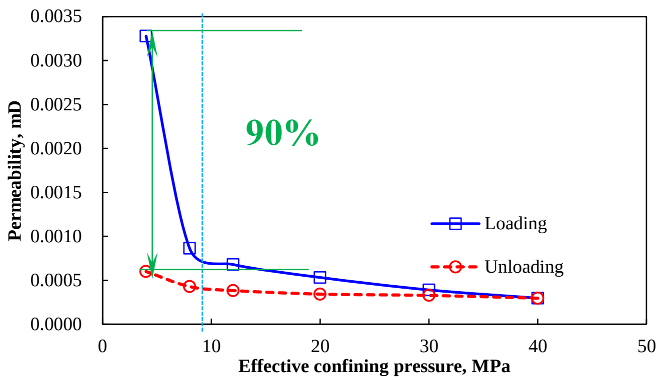

(a)

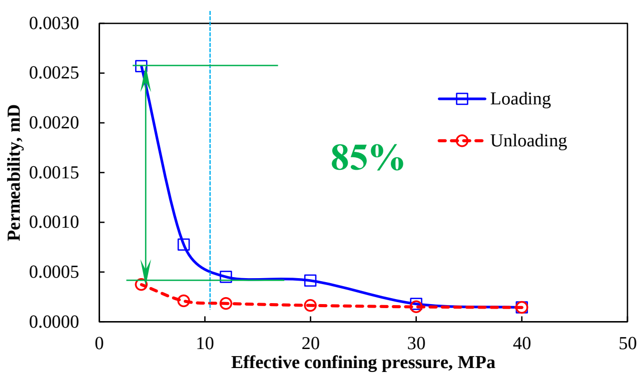

(b)

Fig. 7 The curves of permeability vs. confining pressure: (a) C7-1 sample, (b) C7-2 sample.

3. QUANTITATIVE INTERPRETATION OF STRESS-DEPENDENT PERMEABILITY

3.1. Mathematic model

The tight sandstone contains both pores and microfractures, which result in complex characteristics of stress-dependent permeability (David et al., 1994). To simplify the analytical process, we make the following assumptions:

(1) The pores and microfractures deformation follows the pore elasticity theory.

(2) The pores are considered as many capillary bundles.

(3) The microfractures are regarded as surface plate.

(4)The pore compressibility coefficient is only determined by elastic parameters. The pore geometry has no effects on pore compressibility coefficient (Zhang et al., 2015).

As for dual-porosity medium, the bulk permeability is given by

$$K_t = K_m + K_f \tag{1}$$

$$K_m = \frac{\phi_m r^2}{8}, \quad K_f = \frac{\phi_f w^2}{12}$$

where K_t, K_m and K_f are bulk permeability, matrix pores permeability and microfractures permeability; $\emptyset_m$ and $\emptyset_f$ are the matrix pores porosity and microfractures porosity; r is the pore radius; w is the width of microfractures.

The bulk pore compressibility coefficient is described by

$$C_\phi = \frac{\phi_m C_m + \phi_f C_f}{\phi_m + \phi_f} \tag{2}$$

$$C_m = -\frac{1}{\phi_m}\frac{d\phi_m}{d\sigma}, \quad C_f = -\frac{1}{\phi_f}\frac{d\phi_f}{d\sigma}$$

where $C_\emptyset$, C_m and C_f are bulk pore compressibility coefficient, matrix pores compressibility coefficient and microfractures compressibility coefficient; σ is effective stress.

Mckee et al. (1988) proposed that the stress sensitive coefficient is given by

$$\gamma = -\frac{1}{K_t}\frac{dK_t}{d\sigma} \tag{3}$$

According to Zhang et al.(2015), the stress sensitive coefficient can also be described by

$$\gamma = \alpha C_\phi \tag{4}$$

where γ is stress sensitive coefficient; α is sensitivity exponent.

$$\alpha = \frac{\left(6r^2\phi_m C_m + 6w^2\phi_f C_f\right)\left(\phi_m + \phi_f\right)}{\left(3r^2\phi_m + 2w^2\phi_f\right)\left(\phi_m C_m + \phi_f C_f\right)} \tag{5}$$

Combining Eq.(1), (2), (3) and (4), the sensitivity exponent is given by

$$\alpha = 2\left(1 + \frac{\phi_f}{3\phi_m + 2\phi_f}\right) \tag{6}$$

The pore compressibility can also be expressed by elastic parameters (Wardy et al.,2004).

$$C_\phi = \frac{2(1+\nu)}{E} \tag{7}$$

where E is elastic modulus; ν is Poisson's ratio.

The stress sensitive coefficient is expressed as follows:

$$\gamma = \frac{4(1+\nu)}{E}\left(1 + \frac{\phi_f}{3\phi_m + 2\phi_f}\right) \tag{8}$$

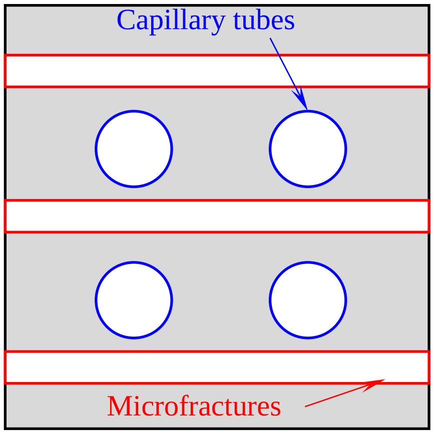

Fig. 8 The schematic illustration of pore structure in tight sandstone.

3.2. Simulation results

(1) Elastic parameters

The elastic parameters (i.e., elastic modulus and Poisson's ratio) have important effects on stress sensitive coefficient. Fig. 9 presents the curves of stress sensitive coefficient vs. Poisson's ratio. A positive relationship is observed. It is worth noting that stress sensitive coefficient does not change too much with Poisson's ratio. It suggests that Poisson's ratio has a weak effect on stress-dependent permeability. Fig. 10 presents the curves of stress sensitive coefficient vs. elastic modulus. The stress sensitive coefficient is negatively related to elastic modulus. The elastic modulus has a strong effect on stress-dependent permeability.

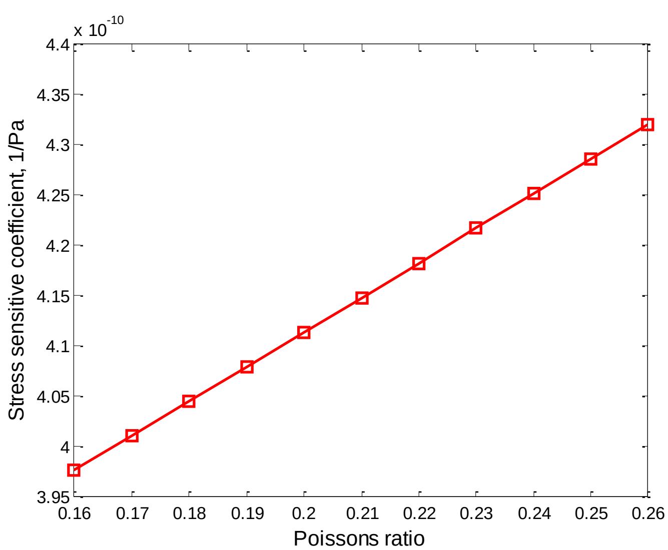

Fig. 9 The relationship between stress sensitive coefficient and Poisson's ratio.

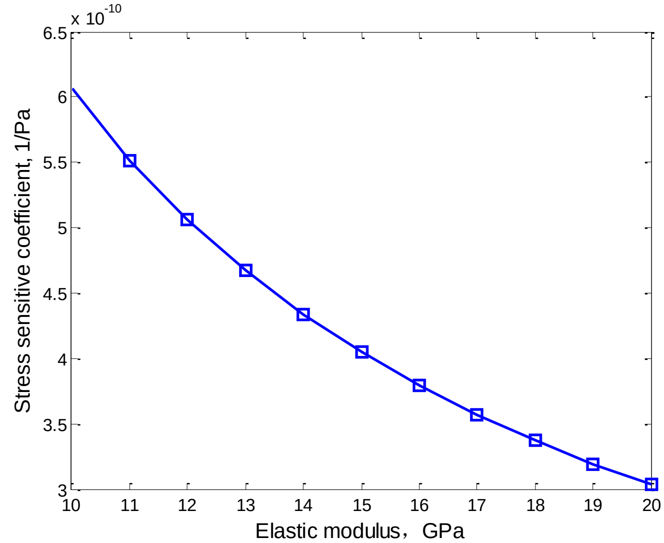

Fig. 10 The relationship between stress sensitive coefficient and elastic modulus.

(2) Pore volume/fracture volume (PV/FV)

The ratio of pore volume to fracture volume (PV/FV) can help develop a quantitative interpretation on the effects of microfractures on stress-dependent permeability. The larger value of PV/FV suggests that the tight sandstone contains fewer microfractures. PV/FV=0 means no pores in samples, and PV/FV=∞ means no fractures in samples. In Fig. 11, it lists the curves of stress sensitive coefficient vs. PV/FV. The stress sensitive coefficient significantly decreases with PV/FV. When the value of PV/FV is larger than 2, the stress sensitive coefficient does not change obviously. It should be noted that the volume fraction of microfractures has an important effects on stress-dependent permeability.

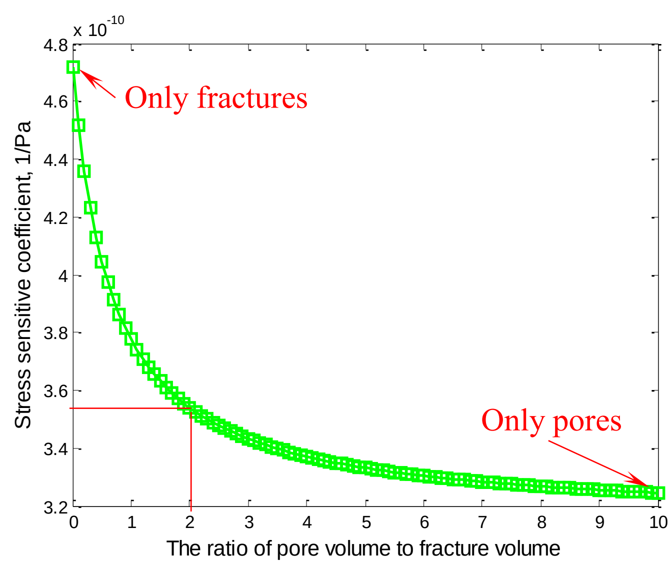

Fig. 11 The relationship between stress sensitive coefficient and PV/FV.

4. CONCLUSIONS

A series of stress-dependent permeability experiments were conducted to study the effects of microfractures in tight sandstone. In addition, the theoretical analysis depending on pore elasticity theory is carried out to explore the related influencing factors. The conclusions are as follows:

(1)Chang-7 formation contains more microfractures than Fuyu formation. The width of microfractures is about 124~253 nm. It is worth noting that the development of microfractures does not result in much larger permeability in Chang-7 formation.

(2)The experimental results show that the permeability damage degree of Chang-7 formation is about 85~90%. It suggests that microfractures deformation cannot recover easily.

(3) The stress sensitive coefficient significantly decreases with PV/FV. When the value of PV/FV is larger than 2, the stress sensitive coefficient does not change obviously. It should be noted that the volume fraction of microfractures has an important effects on stress-dependent permeability. The high microfractures compressibility is the primary reason why the permeability in tight sandstone presents more sensitivity to effective stress.

ACKNOWLEDGEMENTS

The financial support of our shale research program is supported by National Natural Science Foundation of China granted No. 11702296, from National Science and Technology Major Project granted No. 2016ZX05046-003, and funded by China Postdoctoral Science Foundation granted No. 2016M601141.

REFERENCES

Cho, Y., Ozkan, E., Apaydin, O.G., 2013, May 1. Pressure-dependent Natural-fracture Permeability in Shale and its Effect on Shale-Gas Well Production. *Society of Petroleum Engineers*. http://dx.doi.org/10.2118/159801-PA.

Chalmers, G., Ross, D., Bustin, R., 2012. Geological controls on matrix permeability of devonian Gas shales in the Horn River and Liard basins, northeastern British Columbia, Canada. *Int. J. Coal Geology* 103, 120-131.

David, C., Wong, T., Zhu, W., et al., 1994. Laboratory measurement of compaction induced permeability change in porous rocks: implicationsfor the generation and maintenance of pore pressure excess in the crust. *J. Pageoph*. 143, 425-456.

Dong, J.J., Hsu, J.Y., Wu, W.J., et al., 2010. Stress-dependence of the permeability and porosity of sandstone and shale from TCDP Hole-A. *Int. J. Rock Mech. Min. Sci.* 47 (7), 1141-1157.

Gangi, A., 1978. Variation of whole and fractured porous rock permeability with confining pressure. *Int. J. Rock Mech. Mining Sci. Geomech*. Abstracts. 15 (5),249-257.

Jones, F.O., 1975. A Laboratory Study of the Effects of Confining Pressure on Fracture Flow and Storage Capacity in Carbonate Rocks. *SPE 4569*.

McKee, C.R., Bumb, A.C., Koenig, R.A., 1988. Stress-dependent permeability and porosity of coal and other geologic formations. *SPE Form.* Eval. 81-91.

Reyes, L., Osisanya, S.O., 2002. Empirical correlation of effective stress dependent shale rock properties. *J. Can. Petroleum Technol.* 27 (12), 47-53.

Walsh, J.B., 1981. Effect of pore pressure and confining pressure on fracture permeability. *Int. J. Rock Mech. Min. Sci. Geomechanics* Abstr. 18 (5), 429-435.

Wardy, W., 2004. Effective stress law for the permeability of clay-rich sandstones. *J. Geophys. Res*. 109 (B4).

Zhang, R., Ning, Z., Yang, F. et al. 2015. Impacts of nanopore structure and elastic properties on stress-dependent permeability of gas shales. *Journal of Natural Gas Science and Engineering*. 26, 1663-1672.